Supplementary Information for:

Intertrack surface losses in miniature coplanar waveguide on silicon-on-insulator

Jaouad Marzouk, Vanessa Avramovic and Steve Arscott

Institut d'Electronique, de Microélectronique et de Nanotechnologie (IEMN), CNRS UMR8520, The University of Lille, Cité Scientifique, Avenue Poincaré, 59652 Villeneuve d'Ascq, France.

1. Microfabrication of the samples

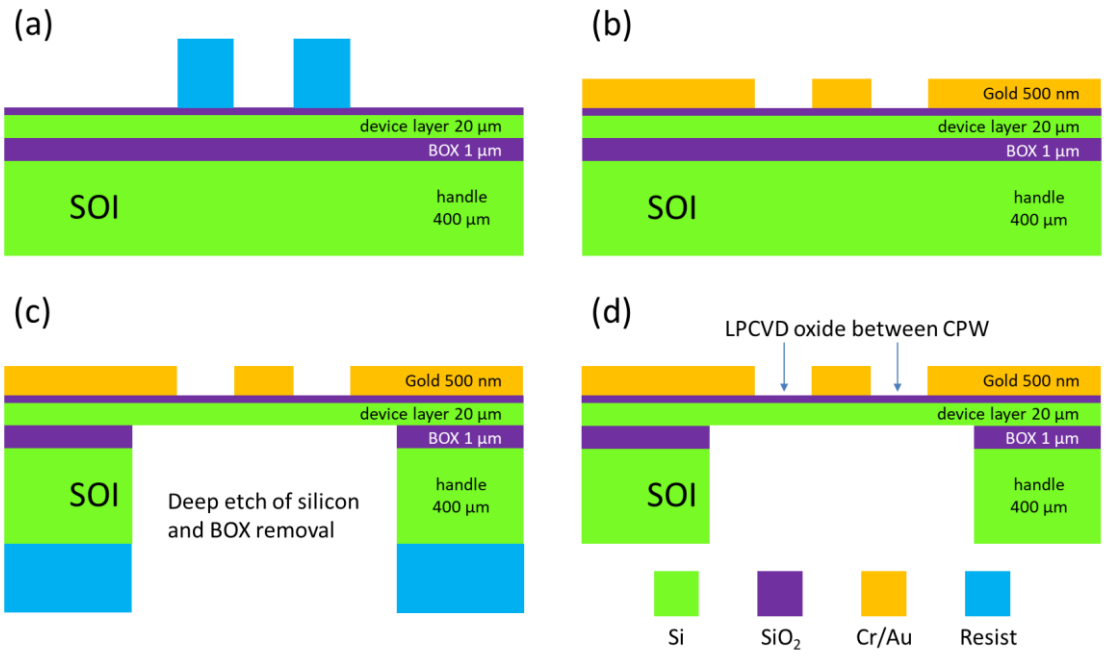

Supplementary Figure 1. Schematic diagram of the major steps of the microfabrication of the miniature, suspended coplanar waveguides. (a) resist mask for lift-off, (b) metallization and lift-off of metal, (c) back-to-front photolithographic alignment for deep-etch mask, and (d) removal, cleaning of CPW in preparation for surface treatments and microwave characterization. Note that step (a) is

preformed twice to provide 1000 µm thick contact pads for the placing of commercial probes. The details of the process can be found in Ref. [1].

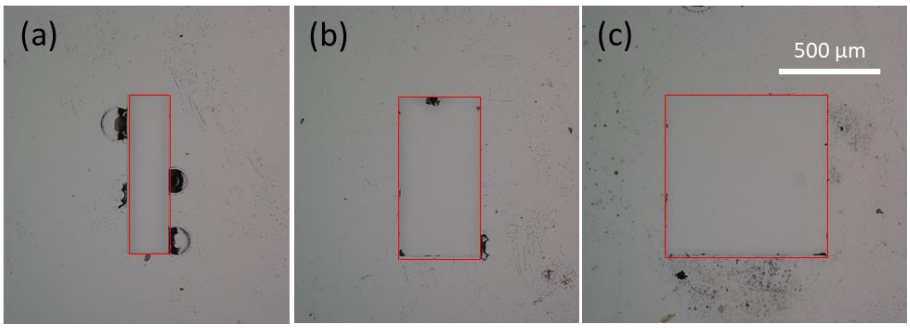

Supplementary Figure 2. Photographic images taken using an optical microscope of the results of the deep back etching of the silicon handle (400 µm). The BOX is visible at the bottom of the deep etch (inside the red quadrilaterals).

2. Return losses (S_{11} and S_{22}) for all microwave measurements

2.1. Return losses for the large-gap CPW

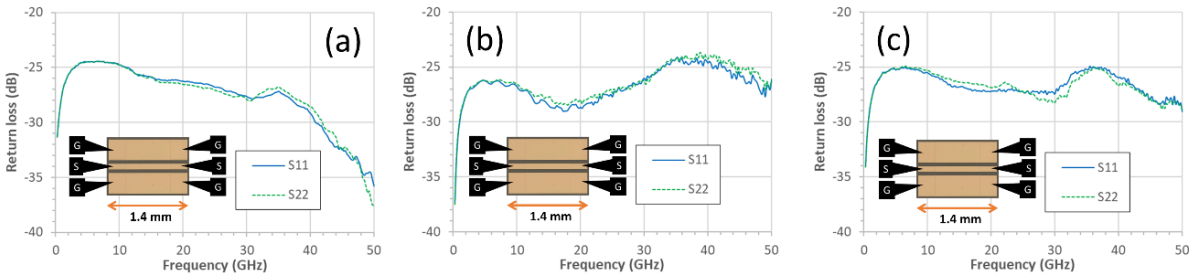

Supplementary Figure 3. Measured Return losses (S_{11} and S_{22}) for the large-gap CPW. (a) With the silicon dioxide present between the CPW tracks, (b) with a hydrogen-terminated silicon surface between the CPW tracks, and (c) with a 3-month-old native oxide on the silicon surface between the tracks.

2.2. Return losses for the transmission lines including the small-gap CPW

2.2.1. Return losses for the miniature CPW a silicon dioxide between the tracks

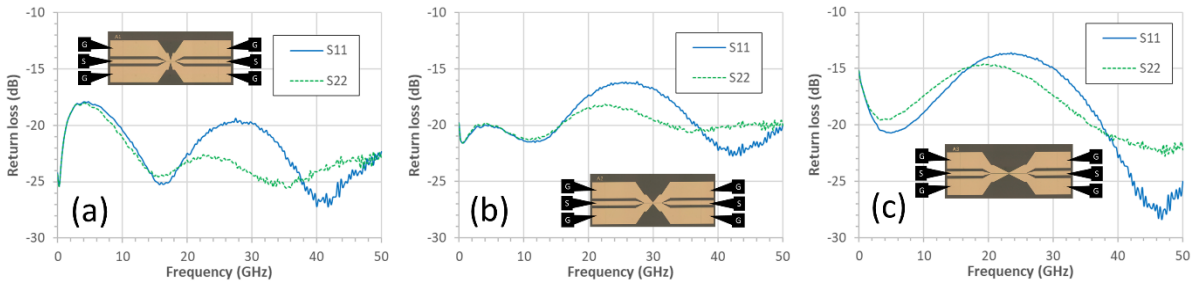

Supplementary Figure 4. Measured Return losses (S_{11} and S_{22}) for the transmission lines including the small-gap CPW with a 50 nm thick silicon dioxide (SiO_2) layer present between the CPW tracks. The small-gap CPW length equals: (a) 200 µm, (b) 400 µm, and 800 µm.

2.2.2. Return losses for the miniature CPW with a hydrogen-terminated surface between the tracks

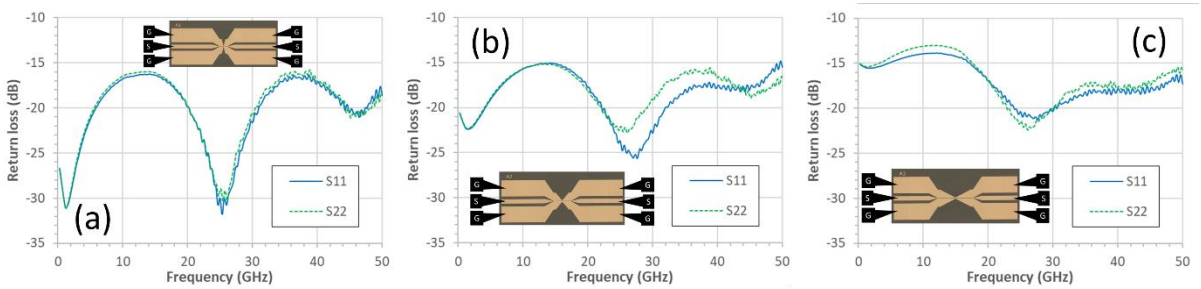

Supplementary Figure 5. Measured Return losses (S_{11} and S_{22}) for the transmission lines including the small-gap CPW with a hydrogen-terminated silicon (Si-H) surface present between the CPW tracks. The small-gap CPW length equals: (a) 200 µm, (b) 400 µm, and 800 µm.

2.2.3. Return losses for the miniature CPW after 3 months native oxide growth on the hydrogen-terminated silicon surface between the tracks

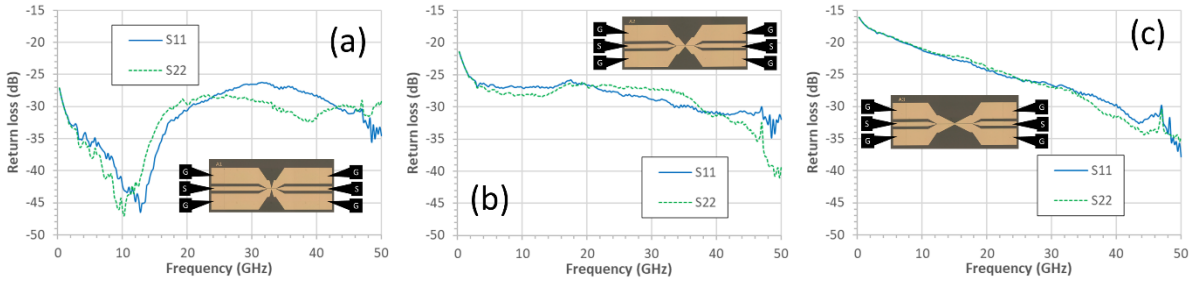

Supplementary Figure 6. Measured Return losses (S_{11} and S_{22}) for the transmission lines including the small-gap CPW with a 3-month-old native oxide (SiO_x) on the silicon surface between the CPW tracks. The small-gap CPW length equals: (a) 200 µm, (b) 400 µm, and 800 µm.

2.2.4. Return losses for the miniature CPW after 5 years native oxide growth on the hydrogen-terminated silicon surface between the tracks

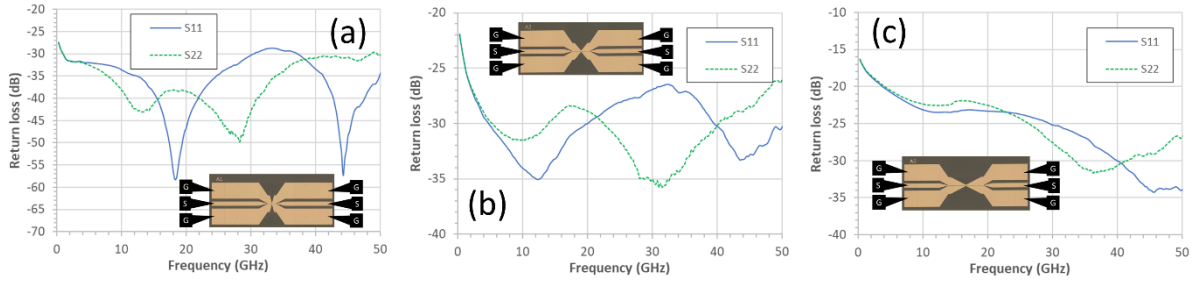

Supplementary Figure 7. Measured Return losses (S_{11} and S_{22}) for the transmission lines including the small-gap CPW with a 5-year-old native oxide (SiO_x) on the silicon surface between the CPW tracks. The small-gap CPW length equals: (a) 200 µm, (b) 400 µm, and 800 µm.

2.2.5. Return losses for the miniature CPW after the 5-year-old native oxide is removed from the hydrogen-terminated silicon surface between the tracks

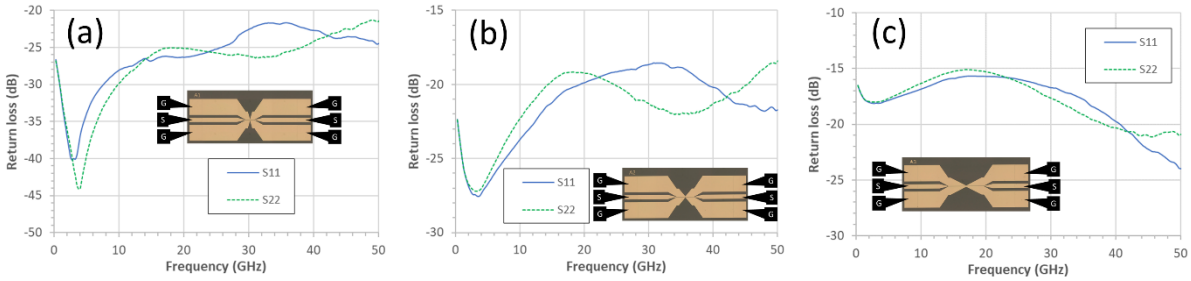

Supplementary Figure 8. Measured Return losses (S_{11} and S_{22}) for the transmission lines including the small-gap CPW with a hydrogen-terminated silicon (Si-H) surface present between the CPW tracks following the removal of the 5-year-old native oxide on the silicon surface between the tracks. The small-gap CPW length equals: (a) 200 µm, (b) 400 µm, and 800 µm.

3. Microscope images of miniature CPW after etching with HF-based solution

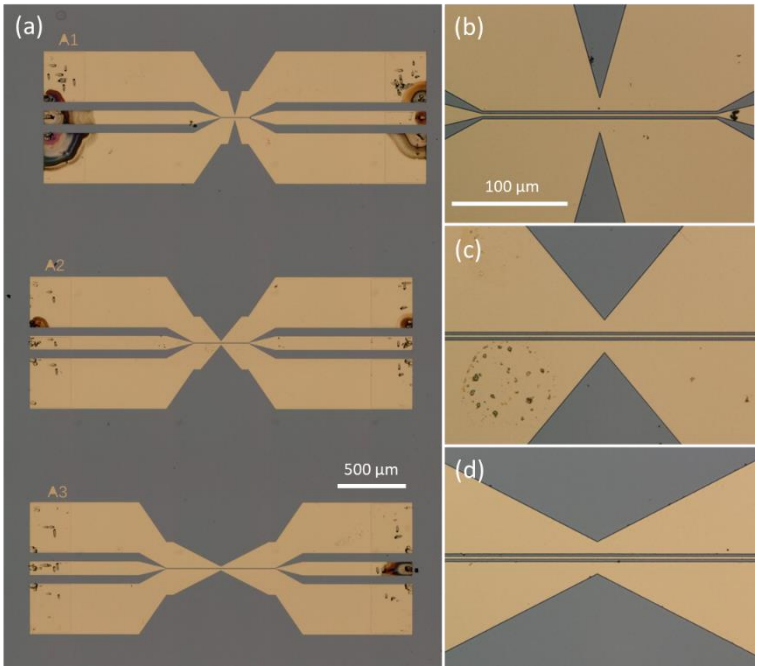

Supplementary Figure 9. Optical microscopy images of examples of transmission lines including the small-gap CPW taken after exposure to the buffered HF solution. Local damage was observed where the commercial microwave probes have previously probed the samples. However, for samples which

had not been previously probes—and for the CPW tracks—no damage was observed (see insets to the figure). The visible damage caused by the HF etching had no effect on the microwave probing.

4. The effect of light on CPW on semiconductor substrates

In our experiments the background irradiance of the samples can be estimated to be of the order of 60 μW cm^{-2}. In terms of lower irradiance, Bhadauria *et al* [2] predict little change in the insertion loss of CPW (on high-resistivity silicon) for an irradiance of ~3 W cm^{-2}. Using high-resistivity silicon (>4000 Ω cm) and a metallization similar to our work, Lee *et al* [3] observed little change of insertion losses of CPW using a lower irradiance of 0.17 W cm^{-2}. However, it has long been known that light can be used to control millimetre-wave propagation [4]. For a CPW patterned onto a semiconducting substrate, incident light can result in the presence of photo-induced free carriers between the CPW tracks [5]. Such free carriers can contribute to losses and result in signal attenuation. Indeed, this effect has been applied for microwave switching. Using CPW on high-resistivity silicon, Platte and Sauerer [5] showed that an optical irradiance (light power per area) of >100 mW cm^{-2} is required to induce a sizeable photo-induced attenuation—achieving ~1.8 dB at 15 GHz. This effect has been applied for the control of microwave circuits based on CPW [6]. Poesen *et al* [7] used an irradiance of 45 W cm^{-2} to induces losses of 40 dB at 100 GHz in CPW on high-resistivity silicon. Using an irradiance of 7 W cm^{-2}, Posen *et al* [8] induced an insertion loss of ~10 dB at 50 GHz. Using an irradiance (532 nm) of 315 μW cm^{-2}, Sameshima *et al* [9] demonstrated that the excess carrier concentration varied depending on the surface—ranging from ~0.5×10^{12} cm^{-3} to ~1.2×10^{13} cm^{-3} for a 'recombination-free' surface.

The number of optically-generated excess free carriers Δn can be estimated using the following relationship [10]:

$$\Delta n = \frac{\alpha I}{hf}(1-R)S\tau_{eff}$$

where α is the absorption coefficient (m^{-1}), I is the irradiance (W m^{-2}) of the incident light, R is the reflectivity of the semiconductor, h is Planck's constant (6.62×10^{-34} Js), f is the frequency (Hz) of the

light, S is the relative spectral response (0.5 for silicon), and τ_{eff} is the effective free carrier lifetime (s) which is given by:

$$\frac{1}{\tau_{eff}} = \frac{1}{\tau} + \frac{2S}{d}$$

Where τ is the lifetime (s) of the carriers in the bulk, d is the thickness (m) of the semiconductor, and S is the surface recombination velocity (m s^{-1}) of the semiconductor surface.

If we consider our high-resistivity (1000 Ω cm) silicon which has a p-type background doping density of 1.47×10^{13} cm^{-3}. The minority (electrons) carrier lifetime in bulk silicon at this doping density is ~1×10^{-3} s [11]. If we consider four wavelengths to approximate the background white light: 400 nm, 500 nm, 600 nm, and 700 nm. The absorption coefficients α and reflectivities R of these wavelengths for silicon are given in the table below.

Table. Absorption coefficients α and reflectivities R of silicon at the four different wavelengths λ considered [12,13].

λ (nm)	α (cm^{-1})	R
400	1×10^{5}	0.5
500	1×10^{4}	0.4
600	5×10^{3}	0.36
700	1×10^{3}	0.34

Using high-resistivity silicon (1000 Ω cm), Mackel and Cuevas [14] measured the surface recombination velocity for hydrogen-terminated silicon to be 5.8 cm s^{-1}, and a native oxide following the HF treatment to be 100 cm s^{-1} after 5½ months in air at room temperature. The above equation can now be used to calculate the effective minority carrier lifetime in the 20 μm thick silicon device layer for and hydrogen-terminated surface and a native oxide which has regrown onto the initially hydrogen-

terminated surface at room temperature in air. The value of τ_{eff} for a hydrogen-terminated silicon surface is 1.47×10^{-4} s, and for a silicon surface having a native oxide, $\tau_{eff} = 9.9\times10^{-6}$ s.

The background irradiance is calculated to be 60 μW cm^{-2}. By using the above equations, the average excess carrier concentration in the first 1 μm thickness of the silicon device layer is calculated to be 4.4×10^{13} cm^{-3} (for the hydrogen-terminated silicon surface) and 3×10^{12} cm^{-3} (for a native oxide 'grown' on an initially hydrogen-terminated silicon surface for several months in air at room temperature).

5. Reasoning behind and derivation of equation 8

The reflected (voltage) waves b at the ports of a two-port network are given in terms of the scattering parameter matrix $\boldsymbol{S}$ and by the incident (voltage) waves a by:

$$\begin{pmatrix} b_1 \\ b_2 \end{pmatrix} = \boldsymbol{S} \begin{pmatrix} a_1 \\ a_2 \end{pmatrix}$$

The scattering parameter matrix of a 2-port transmission line with losses but no reflections is given by:

$$\boldsymbol{S} = \begin{pmatrix} 0 & e^{-\alpha_{Np} l} \\ e^{-\alpha_{Np} l} & 0 \end{pmatrix}$$

where α_{Np} is the Napierian attenuation coefficient of the transmission line, and l is the length along the transmission line.

The forward transmission coefficient S_{21} of the transmission line of length l is thus given by:

$$S_{21} = \frac{b_2}{a_1}$$

Therefore, at a given length:

$$S_{21} = e^{-\alpha_{Np} l}$$

If we choose a unit length l = 1 when comparing two transmission lines (superscripts 1 and 2) of differing attenuation coefficients, we can write:

$$S_{21}^{1} = e^{-\alpha_{Np}^{1}}$$

$$S_{21}^{2} = e^{-\alpha_{Np}^{2}}$$

In each case, the power lost (at length l =1) is:

$$P_{l}^{1} = 1 - (S_{21}^{1})^{2}$$

$$P_{l}^{2} = 1 - (S_{21}^{2})^{2}$$

The ratio of these two lost powers R_{lp}^{21} is:

$$R_{lp}^{21} = \frac{P_{l}^{2}}{P_{l}^{1}} = \frac{1 - e^{-2\alpha_{Np}^{2}}}{1 - e^{-2\alpha_{Np}^{1}}}$$

The Napierian attenuation coefficient α_{Np} (Np per unit length) of the transmission line can be written in terms of the decibel attenuation coefficient α_{dB} using the following relationship:

$$\alpha_{Np} = \frac{\ln 10}{20}\ \alpha_{dB}$$

Therefore:

$$R_{lp}^{21} = \frac{1 - e^{\frac{-\ln 10}{10}\alpha_{dB}^{2}}}{1 - e^{\frac{-\ln 10}{10}\alpha_{dB}^{1}}}$$

Remembering that the superscript of α_{dB} refers to the specific transmission line, i.e. they are not exponentiation.

6. Debye length in the silicon

The Debye length L_D in silicon is given by:

$$L_D = \sqrt{\frac{kT\varepsilon_{Si}\varepsilon_0}{Nq^2}}$$

Where k is Boltzmann's constant ~1.38×10^{-23} JK^{-1}, T is the absolute temperature (here 300K), ε_{Si} is the dielectric constant of silicon (~11.9), ε_0 is the permittivity of free space ~8.85×10^{-12} Fm^{-1}, N is the background doping density of the silicon (1.47×10^{13} cm^{-3}), and q is the elementary charge (~1.6×10^{-19} C).

Using these numerical values, the Debye length in the lightly doped p-type silicon is calculated to be ~1 μm.

Supplementary References

[1] Marzouk J, Arscott S, Fellahi A E, Haddadi K, Lasri T, Christophe Boyaval and Dambrine G 2015 MEMS probes for on-wafer RF microwave characterization of future microelectronics: design, fabrication and characterization *J. Micromechanics Microengineering* **25** 075024

[2] Bhadauria A, Nasimuddin, Verma A K, Sharma E K and Singh B R 2003 Optically controlled microstrip load and stub on silicon substrate *Microw. Opt. Technol. Lett.* **39** 271–6

[3] Lee S, Kuga Y and Mullen R A 2003 Experimental results for a CW-mode optically controlled microwave switch on a silicon-based coplanar waveguide *Microw. Opt. Technol. Lett.* **36** 257–62

[4] Chi Lee, Mak P and DeFonzo A 1980 Optical control of millimeter-wave propagation in dielectric waveguides *IEEE J. Quantum Electron.* **16** 277–88

[5] Platte W and Sauerer B 1989 Optically CW-induced losses in semiconductor coplanar waveguides *IEEE Trans. Microw. Theory Tech.* **37** 139–49

[6] Saddow S E, Thedrez B J and Lee C H 1993 An optoelectronic attenuator for the control of microwave circuits *IEEE Microw. Guid. Wave Lett.* **3** 361–2

[7] Poesen G, Koers G, Stiens J, Carchon G, De Raedt W and Vounckx R 2005 Opto controlled substrate losses in a coplanar waveguide on HR-Si *IEEE MTT-S International Microwave Symposium Digest, 2005.* IEEE MTT-S International Microwave Symposium Digest, 2005. (Long Beach, CA, USA: IEEE) pp 1401–4

[8] Poesen G, Koers G, Stiens J, Carchon G, De Raedt W and Vounckx R 2007 Photo-induced millimeter wave losses in coplanar waveguide on high resistivity silicon *Microw. Opt. Technol. Lett.* **49** 808–10

[9] Sameshima T, Hayasaka H and Haba T 2009 Analysis of Microwave Absorption Caused by Free Carriers in Silicon *Jpn. J. Appl. Phys.* **48** 021204

[10] Platte W 1988 Effective photoconductivity and plasma depth in optically quasi-CW controlled microwave switching devices *IEE Proc. J Optoelectron.* **135** 251

[11] Glunz S W, Rein S, Lee J Y and Warta W 2001 Minority carrier lifetime degradation in boron-doped Czochralski silicon *J. Appl. Phys.* **90** 2397–404

[12] Green M A and Keevers M J 1995 Optical properties of intrinsic silicon at 300 K *Prog. Photovolt. Res. Appl.* **3** 189–92

[13] Green M A 2008 Self-consistent optical parameters of intrinsic silicon at 300K including temperature coefficients *Sol. Energy Mater. Sol. Cells* **92** 1305–10

[14] Mackel H and Cuevas A 2003 Determination of the surface recombination velocity of unpassivated silicon from spectral photoconductance measurements *Proc 3rd World Conf Photovolt Energy Convers* **1** 71–4